ELSEVIER

Catalysis Today 53 (1999) 189–205

CATALYSIS TODAY

www.elsevier.com/locate/cattod

Modeling of the transient sorption and diffusion processes in microporous materials at low pressure

T.A. Nijhuis *, L.J.P. van den Broeke, M.J.G. Linders, M. Makkee, F. Kapteijn, J.A. Moulijn

Delft University of Technology, Department of Chemical Process Technology, Section Industrial Catalysis, Julianalaan 136, 2628 BL Delft, The Netherlands

Abstract

Using pulse-response experiments in an ultra-high vacuum reactor system the adsorption and diffusion behavior of gases in microporous materials can be determined. In a TAP-like system, called Multitrack, the adsorption of gases on zeolites and microporous carbons has been measured. This paper discusses the experimental procedures and the modeling to obtain the relevant sorption and diffusion parameters. Although this technique is macroscopic, contrary to other macroscopic methods such as thermogravimetrical and chromatographic techniques, the diffusivities obtained are in agreement with those determined using microscopic techniques such as NMR. The model used for the description of the measurements is discussed, together with some model simplifications that can be made for special experimental conditions. Possible extensions to the model are also discussed. Finally, the sensitivity of the method towards parameters like sorption strength, diffusion rates, particles size and occupancy range is discussed.

Keywords: Transient sorption; Diffusion; Microporous materials

1. Introduction

Transient measurements in a temporal analysis of products (TAP)-like apparatus can be a very fast and convenient way to determine adsorption and diffusion parameters of components in a porous sorbent particle [1,2]. The advantage of this method is that it is possible to determine the intrinsic properties of a species in one single (pulse) experiment. The disadvantage, however, is that this technique is limited to low partial pressures due to the experimental limitations of the method.

This paper discusses the way in which this type of stimulus–response experiments should be carried out and how to model the experiments accurately to determine the wanted sorption and diffusion parameters.

2. Technique

2.1. Experimental procedure

The sorption experiments in this study were carried out in the so-called Multitrack system. Multitrack, a TAP-like system, was used in the following manner for these experiments. A small (7 mm internal diameter) reactor, containing the sorbent material, is located in an ultra-high vacuum system. To the bottom of this reactor small gas pulses (typically 10^{17} molecules) were fed using high-speed gas pulsing valves. At the reactor exit at the top, the bulk of the gas is removed using a set of skimmers. A small amount of gas

* Corresponding author. Tel.: +31-15-278-6458; fax: +31-15-278-4452

E-mail address: t.a.nijhuis@stm.tudelft.nl (T.A. Nijhuis)

0920-5861/99/$ – see front matter
PII: S0920-5861(99)00116-9

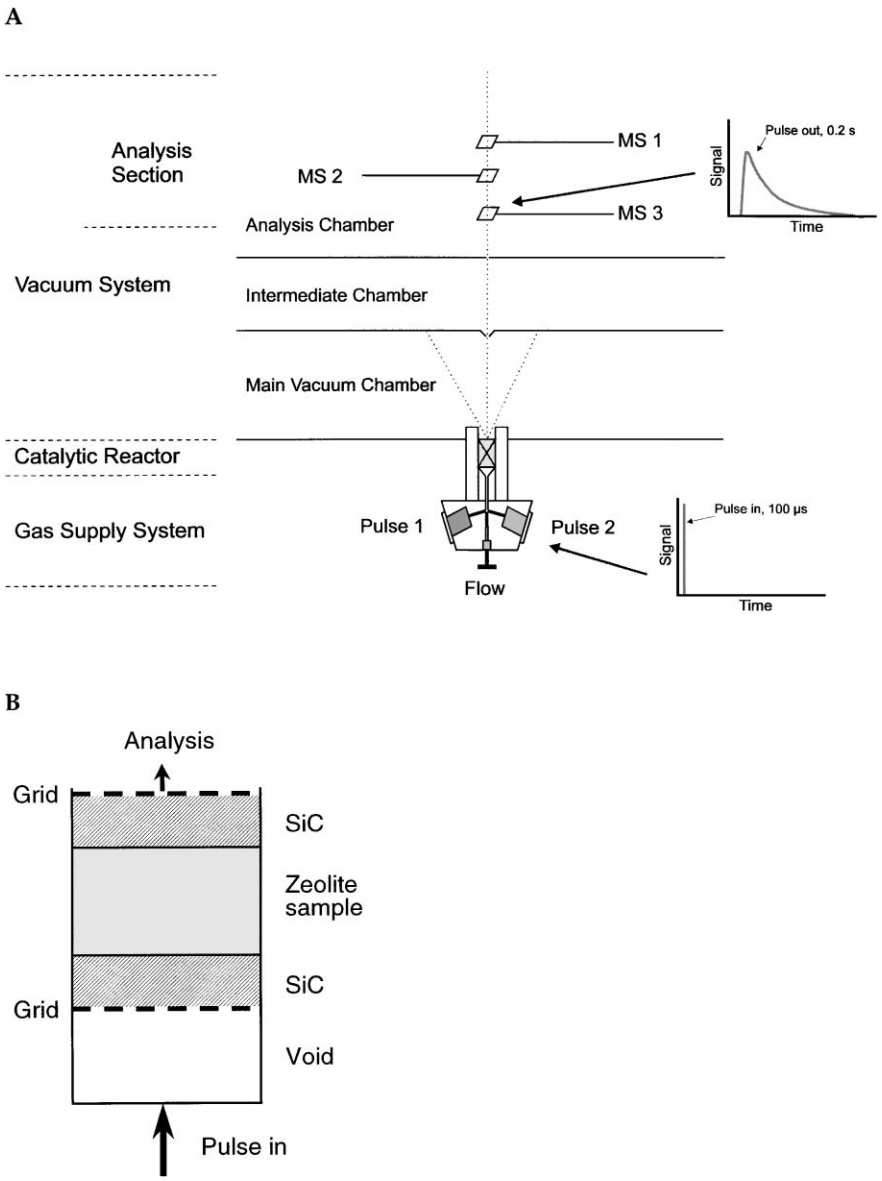

Fig. 1. Schematic representation of the Multitrack system (A) and reactor (B).

travels directly to the analysis section, consisting of three mass spectrometers, which are placed in-line with the skimmers and the reactor outlet. Each of these mass spectrometers is able to measure one component of the gas leaving the reactor with a maximum sampling frequency of 1 MHz. In Fig. 1A Multitrack is schematically represented. A detailed description of Multitrack is available elsewhere [3].

The adsorption experiments were performed with an activated carbon (Sorbonorit B3), silicalite-1, and ZSM-5 (Si/Al = 130) zeolitic material. The zeolites both have a very regular shape with crystals of about 50 μm diameter and 100 μm length. For the carbon a sieve fraction of 105–149 μm was used. The reactor contained about 200 mg of SiC (carborundum) at the bottom on a support grid, in the middle about

200 mg of sorbent, and on top a second layer of about 300 mg of SiC, with a second stainless-steel grid on top to prevent movement of the particles within the reactor. The resulting total bed height in the reactor was always between 10 and 10.5 mm. The reactor is schematically represented in Fig. 1B. The temperature range was varied from ambient temperature up to 773 K. The gas pulse size used was approximately 10^{17} molecules. The gases used were neon and argon (non-adsorbing in this temperature range), and adsorbing gases methane, ethene, propane, *n*-butane, *i*-butane, xenon and carbon dioxide. The purity of all gases used was at least 99.95%. The data-acquisition time of the measurement was set for each of the experiments to measure the entire pulse response, 2 s for pulse-responses of non-adsorbing components, and up to 20 s for pulse-responses of adsorbing components. A sampling frequency of 500 Hz to 2 kHz was used for the mass spectrometers.

2.2. Modeling the experiments

The model used for the description of diffusion through and adsorption and diffusion into sorbent particles is described in detail by Nijhuis [3]. This model is discussed in a condensed form in this subsection.

When modeling gas pulse responses through a packed bed in Multitrack, the transport of gas through the bed can be modeled in rather a simple way because exclusively Knudsen diffusion occurs, since the gas pulses are sufficiently small. Eq. (1) is used to calculate the effective Knudsen diffusivity:

$$D_{\mathrm{K,e}} = \frac{\varepsilon_{\mathrm{b}}}{\tau_{\mathrm{b}}} \times \frac{2\bar{r}}{3} \times \sqrt{\frac{8RT}{\pi M}} \tag{1}$$

For more or less spherical particles the interparticle distance $\bar{r}$ can be calculated from the average particle radius r_{p} using:

$$\bar{r} = \frac{2\varepsilon_{\mathrm{b}}}{3(1-\varepsilon_b)} r_{\mathrm{p}} \tag{2}$$

The bed porosity (ϵ_{b}) and the particle radius (r_{p}) are determined experimentally. The tortuosity (τ_{b}) is obtained from a fitting procedure used in the modeling of the measured pulse responses.

The reactor is divided into four zones. The first zone is an empty space between the reactor bed and the gas pulsing valves, the second an inert SiC zone, followed by the sorbent containing zone, and finally a second inert SiC zone. Each zone is described by its own set of partial differential equations. As mass transport takes place by Knudsen diffusion only, the following differential equation can be used for the gas transport through the reactor (no adsorption):

$$\varepsilon_b \frac{\partial C_z}{\partial t} = D_{\mathrm{K,e}} \frac{\partial^2 C_z}{\partial z^2} \tag{3}$$

Since no particles are present in the first (empty) zone in the reactor, the average characteristic distance in this zone is equal to the inner diameter of the reactor. Since this inner diameter is much larger than the particle diameter in the other zones, the diffusion coefficient in this zone is large compared to the diffusion coefficients in the other zones. It is, therefore, allowed to simplify the model by assuming that this zone is ideally mixed. The concentration in this mixed zone will be set by the amount of gas pulsed and the flux leaving into the first SiC zone. The gas pulses given by the high speed gas pulsing valves have a width at half height of about 100 μs. Since the step size used in the modeling was always larger than 100 ms, it is allowed to consider the entering pulse as a Dirac pulse. This Dirac pulse is incorporated in the model by simply increasing the value of the concentration of the mixed volume with the gas pulse size, at the time the gas pulse is given. The differential equation describing the first mixed zone then becomes:

$$h_{\mathrm{eq}} \frac{\partial C_{\mathrm{m}}}{\partial t} = D_{\mathrm{K,e}} \left. \frac{\partial C_z}{\partial z} \right|_{z=0} \tag{4}$$

This equation can be interpreted as the change in gas concentration in the empty mixed volume section decreasing by the amount of gas diffusing into the first section of the packed bed.

The first of the SiC zones can be described using Eq. (3). As an inlet condition the following equation was chosen:

$$C_z|_{z=0} = f_{\mathrm{c}} C_{\mathrm{m}} \tag{5}$$

A friction factor f_{c} is used to describe the influence of the steel grid supporting the bed. This friction factor is used as a fitting parameter. Although it might be more accurate to derive differential equations across the support grid, it was decided to use this simplification, because the parameters for the diffusion through

the grid can only be roughly estimated. These parameters include the diffusion length due to the varying thickness of the woven material, and the available cross-sectional area for diffusion, because the open space in the grid will be partly unavailable for diffusion, due to the presence of SiC particles. The value of the friction factor was found to vary from 0.3 to 0.8. These values are realistic in view of the very steep concentration gradient at the entrance of the packed bed, and the lower available porosity for diffusion. The friction factor was introduced, as it proved to describe the measured inert pulse-responses better than in the absence of this parameter. Since the aim of this methodology was to determine the adsorption parameters, the exact origin of the entrance resistance was not investigated in detail. At the reactor exit, the concentration profile is generally very flat and the concentrations are extremely low making the necessity for a similar resistance parameter of less significance.

The zone in the middle of the packed bed contains the sorbent material. Eq. (3) should, therefore, be extended with adsorption and desorption terms. In the modeling, adsorption is assumed to occur at the outside of the sorbent particles (or at the exterior of the micropores), followed by diffusion into the interior. The differential equations are:

$$\varepsilon_b \frac{\partial C_z}{\partial t} = D_{K,e} \frac{\partial^2 C_z}{\partial z^2} - k_a N_s C_z (1 - \theta_{z,R}) + k_d N_s \theta_{z,R} \quad (6)$$

$$\frac{\partial \theta_{z,r}}{\partial t} = D_{pore} \nabla^2 \theta_{z,r} \quad (7)$$

with boundary conditions:

$$-D_{pore} a' \cdot \left. \frac{\partial \theta_{z,r}}{\partial r} \right|_{r=R} = k_a C_z (1 - \theta_{z,R}) - k_d \theta_{z,R} \quad (8)$$

$$\left. \frac{\partial \theta_{z,r}}{\partial r} \right|_{r=0} = 0 \quad (9)$$

Eq. (6) represents the gas phase between the particles with adsorption occurring on the outside of the zeolite pores and is identical to Eq. (3) with additional adsorption and desorption terms. Eq. (7) describes the diffusion in the sorbent particles. In this equation both a spherical and a slab geometry was applied in the modeling. For the experiments with the zeolites this provided identical results for both geometries, provided that in the equations the correct specific particle surface area was used. For the more spherical shaped microporous carbon only the spherical geometry was used in Eq. (7). Boundary condition 8 represents the adsorption and desorption of gas, which has to be equal to the amount of gas that diffuses from or to the outside of the sorbent pores. Eq. (9) stands for the symmetry of the concentration profile at the particle center. In these equations it is assumed that there is no interaction between the adsorbed species, which is realistic considering the very low occupancies ($\theta < 0.01$) throughout all experiments performed. The effect of a concentration dependent diffusivity is discussed in the section discussing model extensions. The parameters , k_d, D_{pore}, and N_s are treated as unknown parameters in the modeling.

The third packed bed zone, also containing SiC, can again be described by Eq. (3). The concentration at the start of this zone is equal to the concentration at the end of the sorbent zone. The concentration at the end of the reactor is set to zero. The effect of setting this boundary condition is that no gas leaving the reactor will re-enter the reactor. This is a realistic assumption, considering the low pressure in the main vacuum chamber (and, therefore, at the reactor exit), and the very large pumping capacity maintaining the ultra-high vacuum. The effect on an extension of the model with the concentration in the main vacuum chamber is also discussed later. The flux leaving the reactor (the first derivative of the concentration at the reactor exit) is fitted to the measured pulse responses.

The initial conditions for all equations are that all gas and surface concentrations at the start of the simulation ($t < 0$) are set to zero. The gas pulse is given at $t = 0$. This is simulated by increasing the concentration in the mixed volume by the gas pulse size divided by the volume of the pre-reactor volume instantaneously.

2.3. Solving the differential equations

The differential equations are fitted to the experimental data using a FORTRAN 77 program according to van der Linde et al. [4]. The procedure used for the modeling is described in the next subsection. The set of partial differential equations is discretized according to the ‘numerical method of lines’ using the DSS/2 libraries to give a set of coupled ordinary

differential equations. These equations are integrated using the backward differential formulas method with the LSODES library. Both the DSS/2 and LSODES libraries are described by Schiesser [5]. The amount of gridpoints used for the descretization of the reactor is 101, which are evenly distributed over the three packed bed zones according to the height of the three zones in the reactor. The parameters to be estimated are fitted using the Levenberg–Marquardt method. Using this method the sum of squared residuals (SS-Res) (squared differences between measured and modeled exit concentrations for each timestep of the pulse response) is minimized by changing the parameter values.

A scaling factor is applied to the calculated pulse-response to make the area under the pulse response curve equal to that of the measured pulse-response. The advantage of applying this scaling factor is the absence of a necessity to calibrate the mass spectrometers for the sensitivity of each component. This scaling is allowed provided no irreversible adsorption occurs and no reaction takes place.

2.4. Modeling procedure

The modeling of the pulse responses to obtain the sorption parameters can be divided in two stages. First for each experimental series the bed characteristics (i.e. the transport parameters f_c and τ_b) of the reactor contents have to be determined by fitting the model without adsorption to the pulse response of a non-adsorbing gas. After these parameters are fixed the adsorption parameters can be determined.

The friction factor and the tortuosity are determined by measuring the pulse-responses for a non-adsorbing gas (e.g. neon or argon) over the entire temperature range of the adsorption experiments. The adsorption and desorption rate constant are set to zero and the friction factor and tortuosity are sequentially fitted. The friction factor is then fixed at the average value for all experiments with non-adsorbing gases, and the fitting procedure is then repeated for the tortuosity only. The resulting values for the tortuosity are again averaged, and the tortuosity is then fixed at this value. The averaged friction factor and tortuosity result in a good description of the diffusion through the reactor bed. Fig. 2 demonstrates a calculated pulse-response using these values, together with the corresponding measurement for a pulse of argon over a bed of silicalite-1. The model describes the transport of a non-adsorbing gas through the reactor well. For all adsorption experiments with the same reactor content the two fixed values of f_c and τ_b are used in the determination of the remaining parameters D_{pore}, k_a, and k_d.

The adsorption capacity of MFI zeolites is in the order of 1–2 mmol/g zeolite [6]. Therefore, the amount of gas pulsed is far below the adsorption capacity. This makes it difficult to determine the bed adsorption capacity N_s from the pulse responses for sorbents with an adsorption capacity of this order of magnitude. It is, therefore, more accurate to use an N_s value determined using another technique (e.g. using gravimetric adsorption experiments). The rate constants for adsorption and desorption as well as the diffusivity are determined by fitting the model to the pulse responses measured.

3. Results and discussion of 'standard model'

Fig. 3 shows the pulse-responses of some experiments at different temperatures, in which *n*-butane is pulsed over a sample of silicalite-1, together with the results for the corresponding fits. As can be seen, the model describes the pulse responses accurately. The rate constants obtained from the fitting procedure for a complete experimental series for the adsorption of *n*-butane on silicalite-1 are shown as Arrhenius-plots in Fig. 4. It can be seen that especially for the rate constants for adsorption and desorption the scattering in the datapoints is large. However, if the values for the rate constants for adsorption are compared to the theoretical rate of adsorption, which can be calculated using the kinetic gas theory [3,7], it can be seen that these are in agreement.

The equilibrium constant for adsorption is calculated from:

$$K_{eq} = \frac{k_a}{k_d} \tag{10}$$

The equilibrium constant for adsorption for this method is calculated using concentrations, thermodynamics, however, dictate that one should specify this parameter using (partial) pressures. The calculations are made using concentrations instead of partial

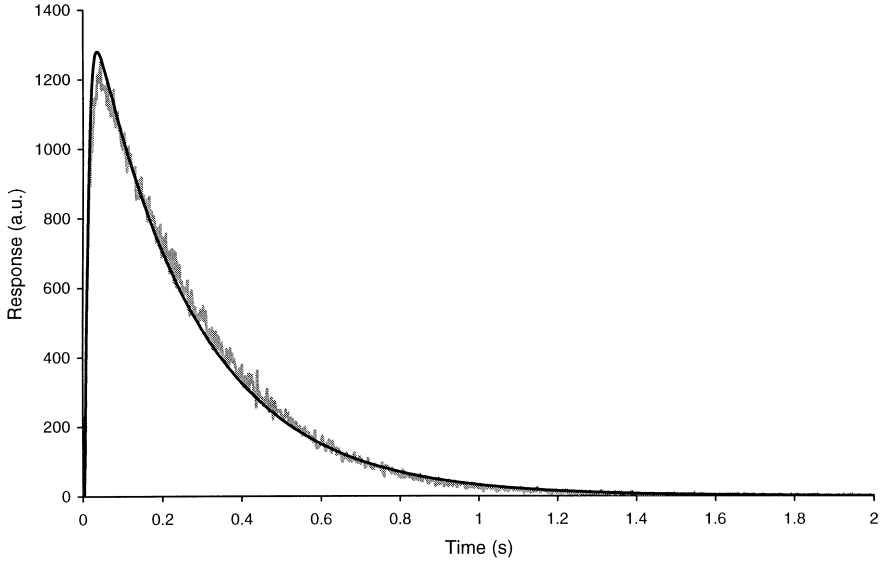

Fig. 2. Measured (gray) and modeled (black) pulse responses for an argon pulse through a bed of in-situ calcined silicalite-1 (473 K).

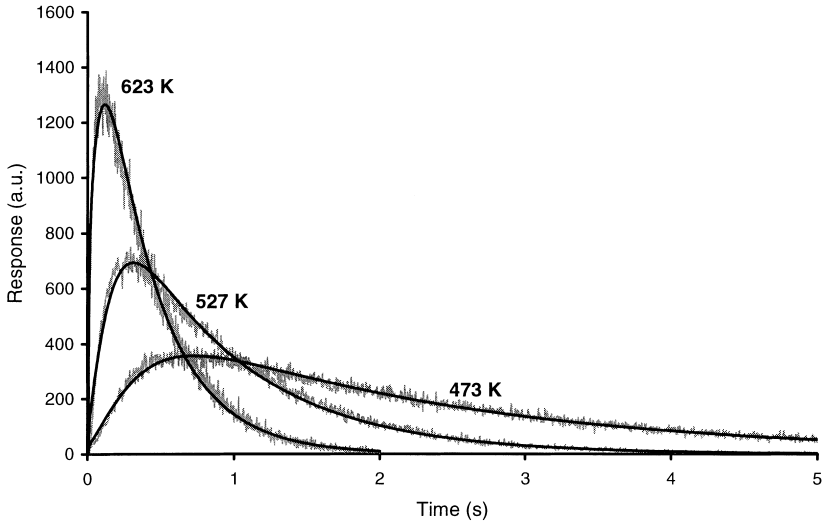

Fig. 3. Measured (gray) and modeled pulse responses (black) for *n*-butane pulses over a bed of in-situ calcined silicalite-1 at 473, 527, and 623 K.

pressures, since this is the more appropriate way to use diffusional equations. The concentration values for the equilibrium constant for adsorption can be converted to partial pressure values using Eq. (11).

$$K_{\mathrm{eq},P} = \frac{K_{\mathrm{eq}}}{RT} \tag{11}$$

In Fig. 5 the van't Hoff-plots are given for the equilibrium constants for adsorption of a number of components on silicalite-1. The scatter, that was present in the values of the rate constants for adsorption and desorption from which the equilibrium constant is calculated, is not present in these graphs. This can be

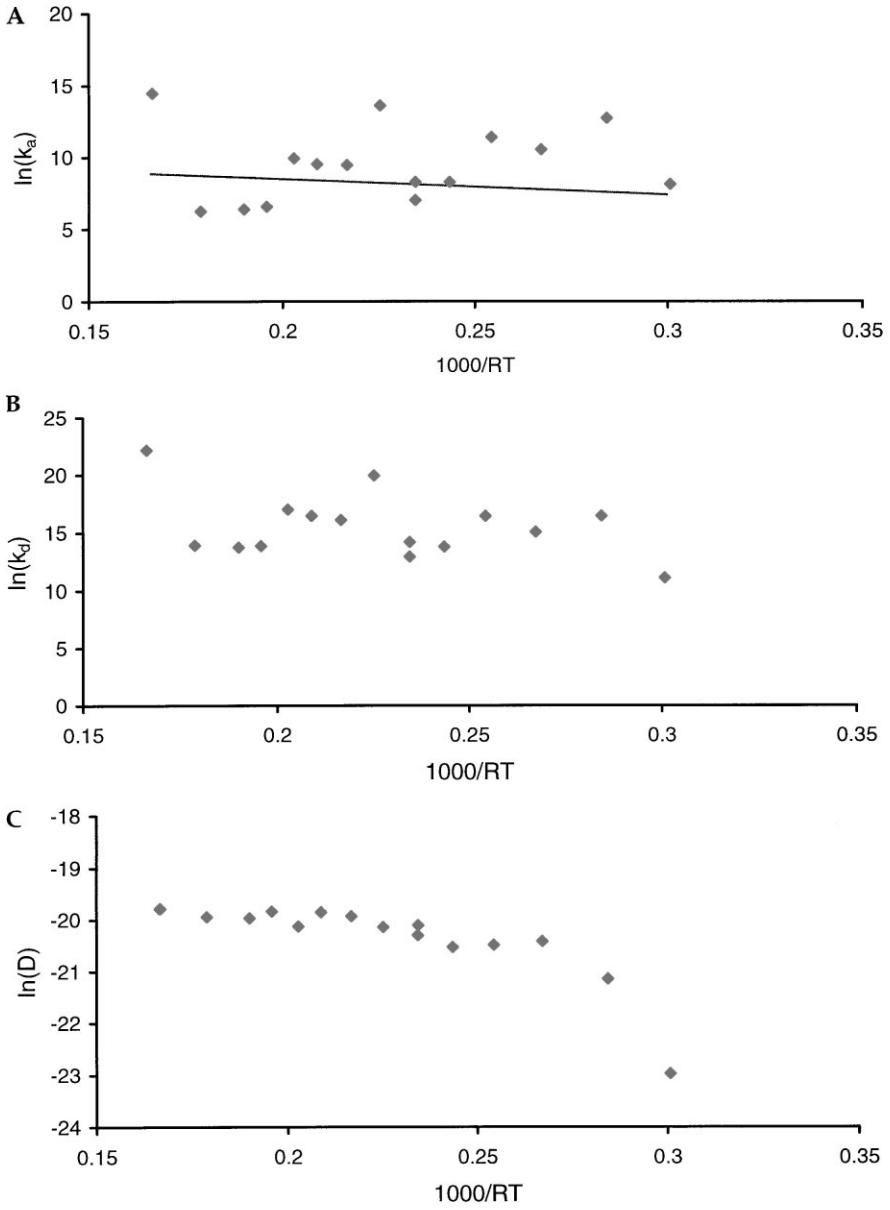

Fig. 4. Van't Hoff- and Arrhenius-plots for the rate constant for adsorption (A), rate constant of desorption (B), and diffusivity (C) of *n*-butane on silicalite-1. The line drawn in figure A shows the theoretical rate of adsorption calculated using the kinetic-gas theory.

explained by the strong correlation in the model that exists between k_a and k_d. This strong correlation makes the model sensitive towards the ratio between these two parameters (i.e. K_{eq}), and less sensitive to the individual values.

In Fig. 5 it can be seen that at high temperatures the datapoints deviate upwards from the trendlines, indicating that at high temperature the fitted model is showing 'too much adsorption' compared to what one would expect from a continuation of the trend of

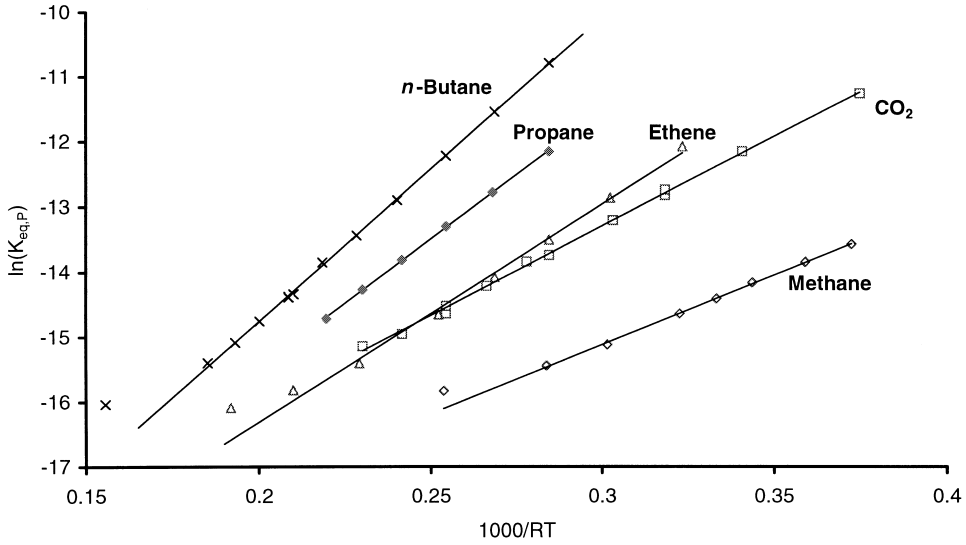

Fig. 5. Van't Hoff-plot of the equilibrium constant for adsorption of measurements for a number of gases on silicalite-1, constructed by calculating the equilibrium constant from the rate constants for adsorption and desorption.

the values at low temperatures. This is due to a slight deviation in the model fit for the non-adsorbing gas (Fig. 2). If one fits the model including adsorption to a pulse response of a non-adsorbing gas, the model calculates that a small amount of adsorption results in the best fit. This amount of adsorption corresponds to approximately $\ln(K_{eq}) = -16.5$, to which all experimental series in Fig. 5 seem to converge at the highest temperatures. The only way to avoid this error is to improve the model for the gas transport through the reactor system. Some possibilities for improvements are discussed later.

In Fig. 6, in which the Arrhenius-plots for the estimated diffusivities are given, again for some data points deviations from the trendlines are visible. In this case these deviations occur both at high and at low temperatures. The deviations at high temperatures can be easily explained, since these diffusivities are calculated while virtually no actual adsorption is occurring, as explained in the previous paragraph. The diffusivity calculated in that case is, therefore, unreliable. The deviations of the calculated diffusivity values from the trendline at low temperatures can be attributed to a lack of sensitivity of the model for the diffusivity in case the adsorption is very strong. The background of this insensitivity is discussed in the paragraph on the applicability of this method.

4. Variations on the basic model

4.1. Model simplifications

The basic model used for the description of the pulse-response sorption–diffusion measurements in the Multitrack system can be simplified in a number of ways. Three simplifications which can be used consecutively will be discussed, together with when these simplifications are allowed and what the consequences are.

4.1.1. Known rate of adsorption

As can be seen in Fig. 4A the model used for the description of the adsorption behavior does not produce an accurate value for the rate constant for adsorption. This can be explained by the strong correlation between the rate constant for adsorption and desorption. For smaller molecules, such as methane, ethane, propane, and *n*-butane, the model produces a rate constant for adsorption that is close to the maximum theoretical rate of adsorption, which can be calculated using the kinetic-gas theory by the collision frequency of the molecules with the (external) sorbent surface. This theoretical rate of adsorption is [8]:

$$r_a = C\sqrt{\frac{RT}{2\pi M}}a'(1-\varepsilon_b) \tag{12}$$

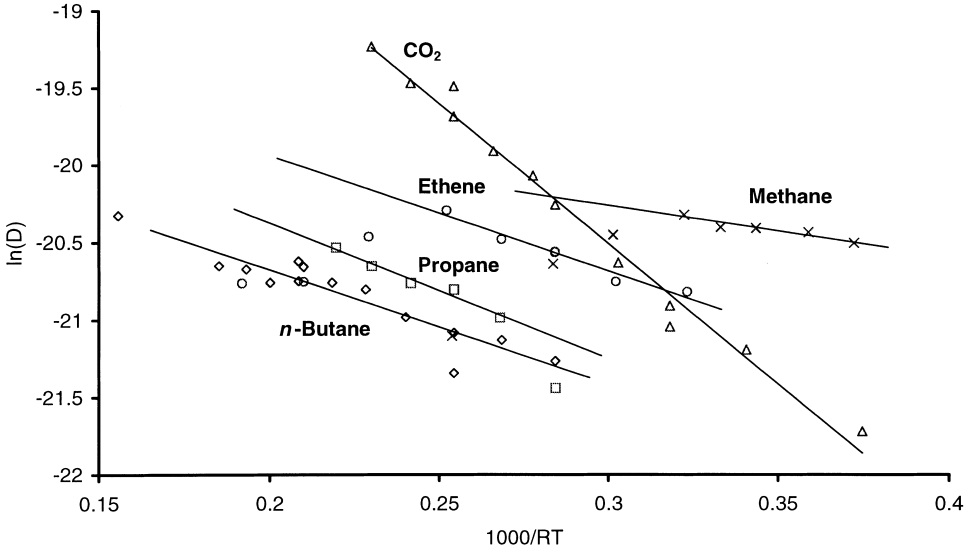

Fig. 6. Arrhenius-plot of the diffusivity for measurements for a number of gases in silicalite-1.

Rearrangement of this equation to obtain a rate constant for adsorption as is used in Eq. (6) leads to:

$$k_a = \frac{1}{N_s}\sqrt{\frac{RT}{2\pi M}}a'(1-\varepsilon_b) \tag{13}$$

If one uses this equation in the model to calculate the rate of adsorption for most light gases good results are obtained. However, if one is fitting a pulse-response for the adsorption of a more bulkier species like *i*-butane in a zeolite like silicalite-1, this method does not produce a modeled pulse response which is able to match the measured pulse-response. If one uses the rate constant for adsorption as a fitting parameter for this case and compares the value obtained to the theoretical rate constant for adsorption as can be calculated using Eq. (13), the fitted value is about a factor of 100 lower. The explanation for this difference can be found in the size of the molecule compared to the pore-size of the zeolite. As the 'large' *i*-butane molecule has difficulty entering the zeolite-pore, not every collision between a gas molecule and the zeolite sorbent will result in a successful adsorption. As a consequence this simplification is limited to molecules having a 'sticking probability' close to 1.

4.1.2. External surface area of sorbent particles at adsorption equilibrium

In most experiments, the rate of adsorption and desorption on the outside of the sorbent particles is very high compared to the diffusion rate into the particle. This diffusion limiting case can be seen as the major reason for the relative insensitivity of the model towards the absolute values of the rate constants for adsorption and desorption. A simplification to the model can, therefore, be to assume the external surface area of the sorbent particles to be at (or very close to) equilibrium with the surrounding gas phase. For very fast diffusing molecules or for very high available adsorption capacities (i.e. high adsorption capacity and high equilibrium constant for adsorption) this simplification does not apply. Also for components having difficulty to enter the sorbent particle, such as is discussed earlier is the case for *i*-butane, this simplification does not apply.

For the assumption of the outside of the sorbent particles being at equilibrium with the surrounding gas-phase, Eq. (6) describing the gas-phase concentration of the sorbent zone in the reactor will change into:

$$\varepsilon_b\frac{\partial C_z}{\partial t} = D_{K,e}\frac{\partial^2 C_z}{\partial z^2} - N_s D_{pore}a'\left.\frac{\partial \theta_{z,r}}{\partial r}\right|_{r=R} \tag{14}$$

The boundary condition for the occupancy at the outside of the sorbent particle, which in this case replaces Eq. (8), now becomes:

$$\theta_{z,r}\big|_{r=R} = \frac{K_{\mathrm{eq}} C_z}{1 + K_{\mathrm{eq}} C_z} \tag{15}$$

4.1.3. Linear driving force (LDF) model

The most drastic simplification that can be used to describe the transient sorption–diffusion in an apparatus like Multitrack is to use a model like the linear driving force (LDF) model, as was first introduced by Glueckauf [9]. In this model a concentration profile in the sorbent particle is not calculated, but a single average occupancy in the particle is used, while the external surface area of the particles is assumed to be at adsorption equilibrium. This simplification drastically reduces the number of differential equations to be solved, as at each axial position now only two concentrations exist (gas-phase + adsorbed), whereas in the complete model at each axial positions in the order of 25 radial concentrations into the particle have to be calculated. In this case the differential equations for the gas phase and adsorbed phase are:

$$\varepsilon_{\mathrm{b}} \frac{\partial C_z}{\partial t} = D_{\mathrm{K,e}} \frac{\partial^2 C_z}{\partial z^2} - N_{\mathrm{s}} D_{\mathrm{pore}} \frac{a'^2}{3} K_{\mathrm{eq}} C_z + N_{\mathrm{s}} D_{\mathrm{pore}} a'^2 \theta_z \tag{16}$$

$$\frac{\partial \theta_z}{\partial t} = D_{\mathrm{pore}} a'^2 K_{\mathrm{eq}} C_z - D_{\mathrm{pore}} \frac{a'^2}{3} \theta_z \tag{17}$$

In Fig. 7A it is shown that even this simplified LDF-type model is able to produce a remarkably good description of the measured pulse responses of *n*-butane over silicalite-1. Although to the eye the two fitted lines have no visible differences, numerically the sum of squared residuals (SSRes) of the LDF-simplified model is 10% higher than the SSRes of the basic model. For most simple adsorption cases this model can be used as a first approximation for the determination of the equilibrium constant for adsorption and the diffusivity, which then can be used as starting values for the full model. Usually the parameter values obtained from the LDF-model and the full model differ only by about 25%. The computing time necessary for the LDF-simplified model is about a factor of 50 less than that for the full model. An easy way to speed up the numerical modeling and to obtain the most accurate parameters is to use this simplified model to gain the starting values for the iterating process of the full model. Fig. 7B shows that for a slow diffusing molecule like *i*-butane the LDF-type model is not able to produce a good experimental fit.

4.2. Model extensions

4.2.1. Exit concentration of the reactor

As discussed the fitting for the model to a pulse-response of a non-adsorbing gas results in an (larger than zero) equilibrium constant for adsorption, while in fact no (measurable) adsorption occurs. This results in the upwards deviating point at high temperatures in the Van't Hoff plot for the equilibrium constant for adsorption. The reason for this virtual adsorption is that the pulse-response of a non-adsorbing gas has more tailing than the transport model predicts. This tailing is partly a result of a non-ideal vacuum system. This non-ideality is caused by a too slow removal of gas from the vacuum chambers. For the main vacuum system this aspect can be modeled by making an extension to the model in which the exit concentration of the reactor is not set to zero, but to set up a mass-balance for the main vacuum chamber. This mass balance is:

$$V_{\mathrm{v}} \frac{\partial C_{\mathrm{v}}}{\partial t} = -\frac{\pi}{4} d_{\mathrm{r}}^2 D_{\mathrm{K,e}} \left.\frac{\partial C_z}{\partial z}\right|_{z=L} - \phi_{\mathrm{v}} C_{\mathrm{v}} \tag{18}$$

The effect of this extension to the model is negligible for most experiments. For experiments in which large (>0.4 mm) particles are used in the reactor, this extension to the model will make a significant improvement. For large particles the gas pulses travelling through the reactor will be narrow (faster diffusion and less uptake area) and as a result a pulse-broadening effect of the vacuum system will be relatively large. The effect of this model extension is very clear when the transport of an argon pulse through a bed of 470 μm Kureha carbon spheres (a carbon molecular sieve) is modeled. The basic model produces a tortuosity of 12 and a friction factor of 1.62 (this value should by definition be between 0 and 1). The extended model on the other hand produces a slightly better fit and more realistic values for tortuosity (5.6) and friction factor (0.76).

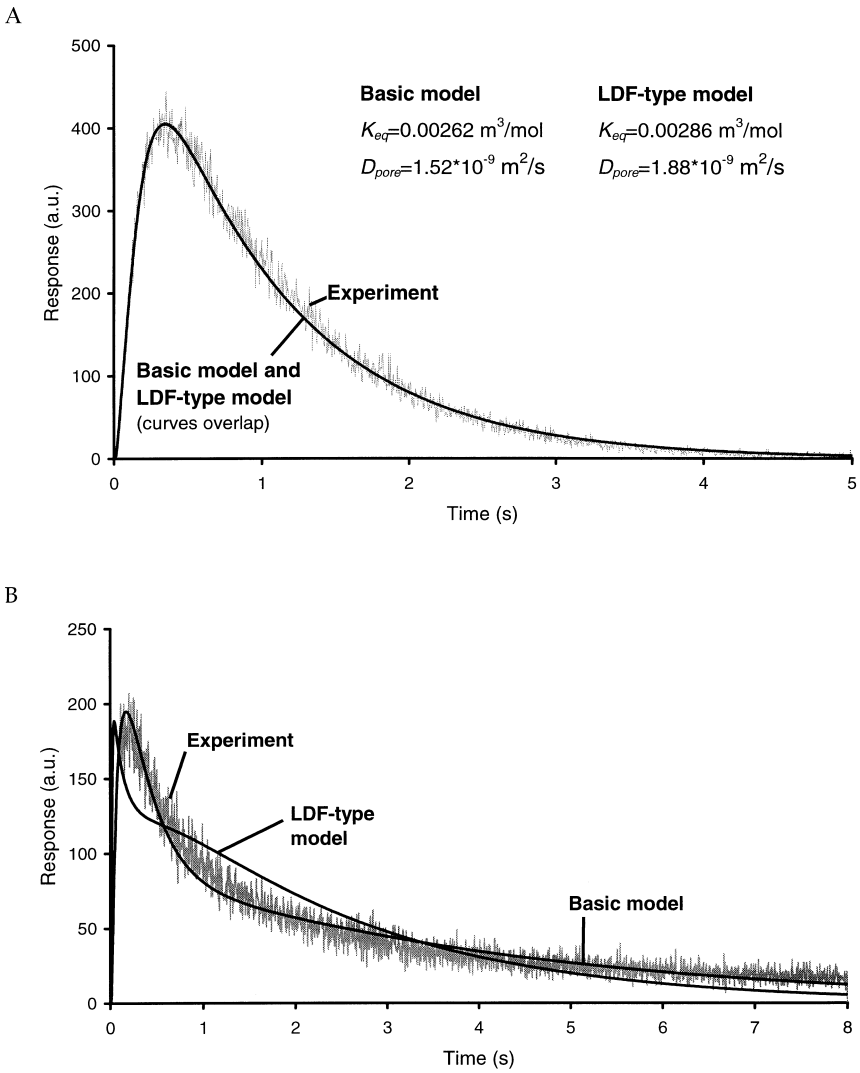

Fig. 7. Comparison for the lines fitted by the basic- and LDF-simplified model to a pulse-response of *n*-butane (A) and *i*-butane (B) over silicalite-1 (513 K).

4.2.2. Concentration dependent diffusivity

In most adsorption experiments in a TAP-like system the occupancies on the sorbent remain very low. Therefore, it is not necessary to use a dependency of the diffusivity on the surface occupancy. Only with very small sample sizes higher occupancies can be reached. For a sample size of 10 mg and an adsorption capacity of 1.5 mmol/g (a typical value for *n*-butane in silicalite-1) a pulse size of 10^{17} molecules can result in a maximum overall occupancy of 0.01. For small zeolite crystals or very fast diffusing components this will hardly show a significant influence on the concentration dependant diffusivity. Large crystals with a slower diffusion can have local higher occupancies (at the outside of the crystals) and have a significant influence on the diffusivity. In the differential Eqs. (7) and (8) the concentration dependency for the diffusion in the particles then should be substituted.

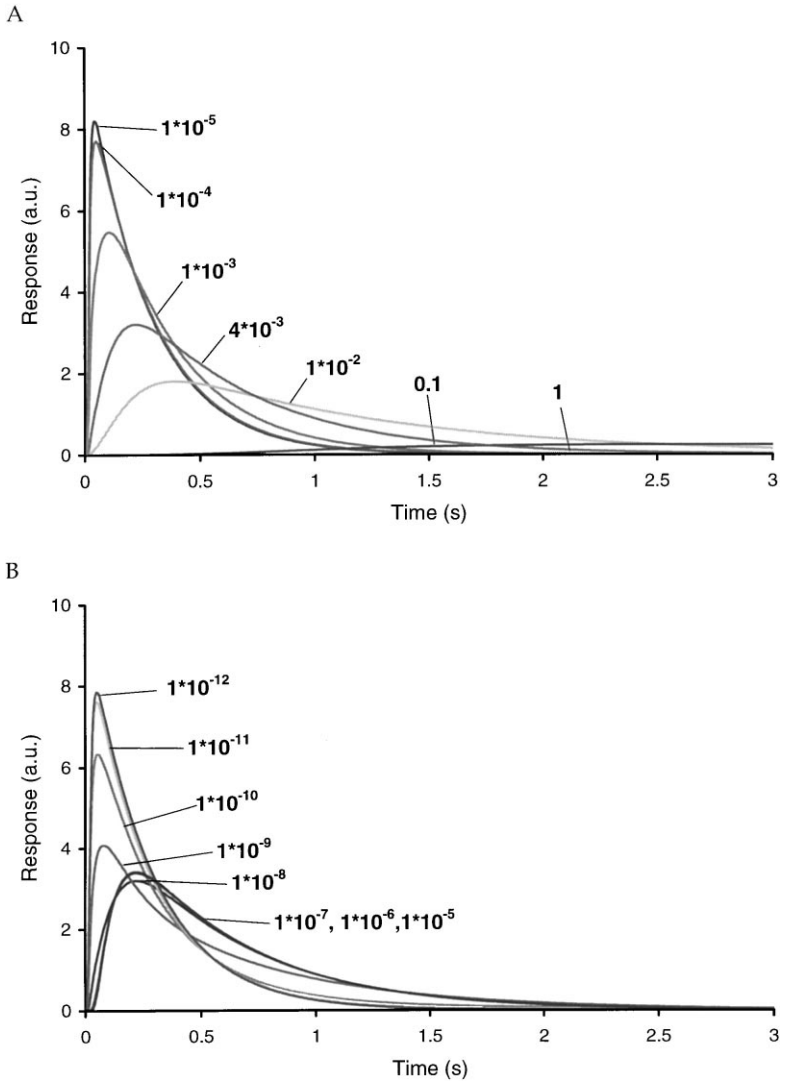

Fig. 8. Sensitivity of model for equilibrium constant for adsorption (A) and diffusivity (B). The pulse responses are calculated for a pulse of *n*-butane over a bed of 200 mg of 50 μm silicalite-1 layered between 230 μm SiC particles (10 mm bed height) at 500 K. A base-case for K_{eq} of 4×10^{-3} mol/m^3 and D_{pore} of 1×10^{-8} m^2/s was chosen. In Figure A the calculated pulse responses different values for K_{eq} (mol/m^3) are shown and in Figure B the calculated pulse responses for different values of D_{pore} (m^2/s) are shown.

5. Model sensitivity

In Fig. 8 the calculated pulse responses are shown for a theoretical pulse of *n*-butane at 500 K travelling through a bed of 200 mg 50 μm silicalite-1 particles layered between 230 μm SiC particles to make a 10 mm total bed height. A fast rate of adsorption (according to the kinetic gas theory was used) and base-case values for the equilibrium constant for adsorption (4×10^{-3} mol/m^3) and diffusivity (1×10^{-8} m^2/s) were chosen. These parameters were then varied around this basic situation. It can be seen that these parameters can be determined over a relatively large range.

The upper limit for the equilibrium constant for adsorption that can be determined is set by the sensi-

tivity of the experimental equipment. In the calculated pulse response for an equilibrium constant for adsorption of 1, the pulse response hardly reaches a significant value and the signal will be lost in the noise that is always present in the measured signal. A very low equilibrium constant for adsorption cannot be determined, since the signal then is almost identical to that of a non-adsorbing gas. It is possible to extend the range over which the equilibrium constant for adsorption can be determined by using a different amount of sample. A larger sample allows for the determination of smaller equilibrium constants for adsorption, the maximum amount of sample (1.5 g) is, however, limited by the physical size of the reactor. Larger equilibrium constants for adsorption can be determined by using smaller sorbent samples. The minimum amount of sample that can be used is around 10 mg, smaller samples will show bypassing of gas along the sorbent in the reactor. These variations in sample size can stretch the range over which the equilibrium constant for adsorption can be determined upwards and downwards by an order of magnitude.

The limits for the diffusivities that can be determined are set by the relative time constant of the diffusion into the particles compared to the time constant of the diffusion through the sorbent bed. Expressions for the time constants for diffusion and transport trough the bed are given in Eqs. (19) and (20).

$$t_{\text{diff}} = \frac{r_{\text{p}}^2}{D_{\text{pore}}} \tag{19}$$

$$t_{\text{trans}} = \frac{L_{\text{bed}}^2}{D_{\text{K,e}}} \propto \frac{L_{\text{bed}}^2}{r_{\text{p}}} \tag{20}$$

A large diffusivity will result in a uniform occupancy across the sorbent particle and cannot be determined. A very small diffusivity will have sharp concentration profiles in the particles and limit the amount of gas that can be adsorbed (the exterior is then at equilibrium with the surrounding gas phase and does not adsorb more gas than is diffusing inwards). If the diffusivity is too small the slower release of gas (tailing of the pulse responses) will be lost in the signal noise and the diffusivity can no longer be determined. The range over which the diffusivity can be determined can be extended easily. The model is most sensitive for the diffusivity if the time-constants for the transport through the bed and for the diffusion into the particles are in the same order of magnitude. Smaller diffusivities can, therefore, be determined by using smaller sorbent particles. The limitation in this case is that smaller particles will produce a wider pulse response due to the smaller Knudsen diffusivity, which will make the noise larger compared to the signal height. The minimum particle size that can be used is about 10 μm. Alternatively the size of the sorbent particles can be made smaller, without making the particles in the bed smaller. This can be done, for example, by coating (gluing) the sorbent particles on small glass beads. Larger diffusivities can be determined by using larger sorbent particles. The only limitation in this case is that the particle size should remain small compared to the reactor diameter to avoid radial profiles over the sorbent bed.

6. Results — comparison with other techniques

6.1. Equilibrium constant for adsorption

From the equilibrium constants for adsorption determined in the adsorption/diffusion experiments, the heat of adsorption and pre-exponential factors $K_{\text{eq,P}}^0$ can be determined by fitting Eq. (21) through a van't Hoff plot as is given in Fig. 5. The results are given in Table 1.

$$K_{\text{eq,P}} = K_{\text{eq,P}}^0 \text{e}^{-\Delta H_{\text{ads}} RT} \tag{21}$$

In Table 2 a comparison between the values determined in this manner and values reported in literature is made. It can be seen the values are in good agreement.

6.2. Diffusivity

The activation energy for diffusion can be determined from the Arrhenius-plot given in Fig. 6 using Eq. (22).

$$D_{\text{pore}} = D_{\text{pore}}^0 \text{e}^{-E_{\text{diff}}/RT} \tag{22}$$

In Table 3 the activation energies for diffusion and the pre-exponential factors detemined using this method are given. In Table 4 the activation energies for diffusion determined using other techniques are given.

Table 1
Overview of determined heats of adsorption and pre-exponential factors for the equilibrium constant for adsorption

Gas	Sorbent	K_{eq}^{0} (10^{-12} 1/Pa)	Heat of adsorption (kJ/mol)
Methane	Silicalite-1[a]	444	21.4
Ethene	Silicalite-1[a]	91.0	33.5
Propane	Silicalite-1	29.7	39.6
	Silicalite-1[a]	73.0	39.4
n-Butane	Silicalite-1	11.1	47.1
	Silicalite-1[a]	33.5	46.8
	Sorbonorit B3	1480	54.1
I-Butane	Silicalite-1	5.47	47.9
Carbon dioxide	Silicalite-1[a]	446	27.5
	Na-ZSM-5 (130)	2.82	44.8
Xenon	Silicalite-1	84.0	29.0

[a] In-situ calcined.

Table 2
Comparison between heats of adsorption determined using different techniques

Gas	Sorbent	This study	Literature	Reference
Methane	Silicalite-1	21.4	18.6	[10]
			18.4	[11]
			20.0	[12]
			20.5	[13]
			21	[14]
			18.6	[15]
Ethene	Silicalite-1	33.5	26.5	[11]
Propane	Silicalite-1	39.4–39.6	37.8	[16]
			40.5	[13]
			41	[14]
			40.9	[15]
n-Butane	Silicalite-1	46.8–47.1	49.4	[13]
			50.5	[14]
			53.0	[15]
	Sorbonorit B3	44.1	50.4	[a]
i-Butane	Silicalite-1	47.9	48.5	[13]
			42	[17]
			56.5	[14]
			47.5	[15]
Carbon dioxide	Silicalite-1	27.5	24.0	[10]
			21.7	[11]
			24.6	[12]
			28.5	[14]
Carbon dioxide	Na-ZSM-5 (Si/Al = 30)	44.8	42.0	[11]

[a] Determined in the scope of study using independant thermogravimetrical experiments.

There is a large difference between the reported values. If one not only considers the activation energies for diffusion, but also at the absolute values of the diffusivities [1,21,27,30], it can be seen that these values can be roughly divided in two groups. The first group contains the values determined using microscopic techniques. These techniques generally yield high diffusivities and low activation energies for diffusion. The other group (macroscopic techniques) generally have high activation energies for diffusion and diffusivities up to two-orders of magnitude smaller than those using microscopic techniques. An explanation for this

Table 3
Overview of determined activation energies for diffusion and pre-exponential factors for the diffusivity of gases in a sorbent

Gas	Sorbent	D^0_{pore} (10^{-9} m^2/s)	E_{diff} (kJ/mol)
Methane	Silicalite-1[a]	4.03	3.1
Ethene	Silicalite-1[a]	9.72	7.5
Propane	Silicalite-1	4.87	7.2
	Silicalite-1[a]	8.07	8.7
n-Butane	Silicalite-1	9.01	7.3
	Silicalite-1[a]	4.56	7.4
	Sorbonorit B3	184	30.0
i-Butane	Silicalite-1	61.1	28.9
Carbon dioxide	Silicalite-1[a]	285	18.1
	Na-ZSM-5 (130)	458	21.8
Xenon	Silicalite-1	228	14.4

[a] In-situ calcined.

Table 4
Overview of reported activation energies for diffusion determined using different techniques

Gas	Sorbent	Literature	Reference	Technique
Methane	Silicalite-1	3.1	this study	Multitrack
		4.0	[18]	PFG-NMR[a]
		16.5	[19]	CPC
		22	[17]	CPC
		5.1	[20]	Membrane
		6.3	[21]	Membrane
Propane	Silicalite-1	7.2	this study	Multitrack
		6.7	[22]	FR
		13.0	[23]	ZLC
		25.6	[19]	CPC
		45	[17]	CPC
		21.8	[24]	FR
		37	[22]	FR
		8	[20]	Membrane
		18.7	[21]	Membrane
		5	[25]	QENS[a]
		6	[26]	PFG-NMR[a]
n-Butane	Silicalite-1	7.3	this study	Multitrack
		8.1	[27]	PFG-NMR[a]
		13.7	[28]	Membrane
		10	[20]	Membrane
		52	[17]	CPC
		21.5	[29]	FR
		21.0	[21]	Membrane

[a] Microscopic methods.

discrepancy is that the macroscopic methods also include the different steps occurring before the actual diffusion of the molecules in the micropores. External transport limitations can, therefore, easily influence the diffusivities. Microscopic methods measure the actual movement of the diffusion molecules in the micropores and, therefore, cannot be influenced by processes outside the sorbent particles, provided long range effects are excluded [27].

The Multitrack method for the determination of the diffusivity in microporous materials is a macroscopic technique, as the measurements include the transport

of the molecules through the bed and into the particles. The results obtained using this method are, however, in excellent agreement with those using microscopic techniques, both for the activation energies for diffusion and for the absolute values for the diffusivities. This can be easily explained since the transport of gas through the bed is by Knudsen-diffusion only and as a result external transport limitations cannot be present.

7. Conclusions

Using the presented low-pressure pulse-response method intrinsic diffusion and adsorption parameters of gases in microporous materials can be determined. The values obtained for these parameters are in good agreement with those determined using microscopic techniques like Pulse-Field-Gradient NMR or QENS.

8. Notation

a'	specific surface area sorbent particle ($m^2_{\text{external surface}}/m^3_{\text{particle}}$)
C	gas concentration (mol/m^3)
C_m	gas concentration in pre-bed empty volume (mol/m^3)
C_v	gas concentration in main vacuum chamber (mol/m^3)
C_z	gas concentration at axial position z (mol/m^3)
d_r	diameter of reactor (m)
$D_{K,e}$	effective Knudsen diffusivity in bed (m^2/s)
D_{pore}	diffusivity in sorbent (m^2/s)
D^0_{pore}	pre-exponential factor diffusivity in sorbent (m^2/s)
E_{diff}	activation energy for diffusion (J/mol)
f_c	friction factor (–)
ΔH_{ads}	adsorption enthalpy (J/mol)
h_{eq}	equivalent height of empty pre-bed volume (pre-bed volume divided by reactor cross section) (m)
k_a	rate constant for adsorption (m^3/mol/s)
k_d	rate constant for desorption (1/s)
K_{eq}	equilibrium constant for adsorption (m^3/mol)
$K_{eq,P}$	equilibrium constant for adsorption (1/Pa)
$K^0_{eq,P}$	pre-exponential factor eq. const. for adsorption (1/Pa)
L_{bed}	height of bed of sorbent material (m)
L_{diff}	diffusion length (m)
N_s	number of adsorption sites per bed volume (mol/m$^3_{bed}$)
M	molar mass of component (kg/mol)
r	radial position in sorbent particle (m)
$\bar{r}$	average interparticle distance (m)
r_a	rate of adsorption (mol/m^3/s)
r_p	average particle size (radius) (m)
R	gas constant = 8.314 (J/mol/K)
t	time (s)
T	temperature (K)
V_v	volume of main vacuum chamber (m^3)
z	axial position (m)
δ	diffusion length for diffusion in zeolite pore (m)
ϵ_b	bed porosity (m^3_{void}/m^3_{bed})
θ	adsorbate occupancy ($sites_{occupied}/sites_{total}$)
θ_z	adsorbate occupancy at axial position z ($sites_{occupied}/sites_{total}$)
$\theta_{z,r}$	adsorbate occupancy at axial position z and radial position r ($sites_{occupied}/sites_{total}$)
ϕ_v	pumping rate from main vacuum chamber (m^3/s)
τ_b	bed tortuosity (–)

References

[1] T.A. Nijhuis, L.J.P. van den Broeke, J.M. van de Graaf, F. Kapteijn, M. Makkee, J.A. Moulijn, Chem. Eng. Sci. 52 (1997) 3401.

[2] O.P. Keipert, M. Baerns, Chem. Eng. Sci. 53 (1998) 3623.

[3] T.A. Nijhuis, Towards a new propene epoxidation process – Transient adsorption and kinetics measurements applied in catalysis, Ph.D. Thesis (in English), Delft University of Technology, Delft, 1997.

[4] S.C. van der Linde, T.A. Nijhuis, F.H.M. Dekker, F. Kapteijn, J.A. Moulijn, Appl. Catal. A: General 151 (1997) 27.

[5] W.E. Schiesser, The Numerical Method of lines — Integration of partial differential equations, Academic Press, London, 1991.

[6] H.B. Abdul-Rehman, M.A. Hasanain, K.F. Loughlin, Ind. Eng. Chem. Res. 29 (1990) 1525.

[7] T.A. Nijhuis, L.J.P. van den Broeke, M.J.G. Linders, J.M. van de Graaf, F. Kapteijn, M. Makkee, J.A. Moulijn, Chem. Eng. Sci. 54 (1999) 4423.

[8] P.W. Atkins, Physical Chemistry, Oxford University Press, Oxford, 3rd ed., 1987, p. 764.
[9] E. Glueckauf, Trans. Faraday Soc. 51 (1955) 1540.
[10] T.C. Golden, S. Sircar, J. Coll. Interf. Sci. 162 (1994) 182.
[11] V.R. Choudhary, S. Mayadevi, Sep. Sci. Technol. 28 (1993) 2197.
[12] L.V.C. Rees, P. Brückner, J. Hampson, Gas Sep. Purif. 5 (1991) 67.
[13] J.R. Hufton, R.P. Danner, AIChE J. 39 (1993) 954.
[14] M.S. Sun, D.B. Shah, H.H. Xu, O. Talu, J. Phys. Chem. B 102 (1998) 1466.
[15] W. Zhu, J.M. van de Graaf, L.J.P. van de Broeke, F. Kapteijn, J.A. Moulijn, Ind. Eng. Chem. Res. 37 (1998) 1934.
[16] J.A. Hampson, L.V.C. Rees, J. Chem. Soc., Faraday Trans. 86 (1993) 3169.
[17] A.S. Chiang, A.G. Dixon, Y.H. Ma, Chem. Eng. Sci. 39 (1984) 1461.
[18] J. Caro, M. Bülow, W. Schirmer, J. Kärger, W. Heink, H. Pfeifer, S.P. Sdanov, J. Chem. Soc., Faraday Trans. I 81 (1985) 2541.
[19] J.R. Hufton, R.P. Danner, AIChE J. 39 (1993) 962.
[20] M.S. Sun, O. Talu, D.B. Shah, AIChE J. 42 (1996) 3001.
[21] J.M. van de Graaf, Permeation and separation properties of supported silicalite-1 membranes — A modeling approach. Ph.D. Thesis (in English), Delft University of Technology, Delft, 1999.
[22] N. van den Begin, L.V.C. Rees, J. Caro, M. Bülow, Zeolites 9 (1989) 287.
[23] M. Eic, D.M. Ruthven, Stud. Surf. Sci. Catal. 49 (1989) 897.
[24] L. Song, L.V.C. Rees, Microporous materials 6 (1996) 363.
[25] H. Jobic, M. Bee, G.J. Kearley, Zeolites 12 (1992) 146.
[26] W. Heink, J. Kärger, H. Pfeifer, J. Chem. Soc., Faraday Trans. 88 (1992) 3505.
[27] J. Kärger, D.M. Ruthven, Diffusion in zeolites and other microporous solids, Wiley/Interscience, New-York, 1992, p. 375.
[28] A. Paravar, D.T. Hayhurst, Direct measurement of diffusivity for butane across a single large silicalite crystal, Proc. 6th Int. Conf. on zeolites — Reno 1983, Butterworth, Guildford, 1983, p. 217.
[29] N. van den Begin, L.V.C. Rees, Stud. Surf. Sci. Catal. 49 (1989) 915.
[30] F. Kapteijn, W.J.W. Bakker, G. Zheng, J.A. Moulijn, Microporous Materials 3 (1994) 227.